(Received 17 May 2025, Accepted 17 July 2025, Scheduled 1 August 2025)

Enhanced Spiral Antenna Performance by Multistep Ground Plane Reflector for 2–18 GHz Applications

Abhay M. Morey[1, *], Avinash R. Vaidya[1], and Sandeepak S. Kakatkar[2]

[1] *Department of Electronics Engineering, Pillai College of Engineering, New Panvel, University of Mumbai, Mumbai-41206, India*
[2] *Society for Applied Microwave Electronics Engineering and Research, Mumbai-400076, India*

ABSTRACT: This paper proposes a multistep reflector backing for compact spiral antennas to provide a consistent unidirectional pattern over a wide frequency band with improved gain, axial ratio (AR), and efficiency for 2–18 GHz applications. The effect of varying the step number and step sizes of the reflector on antenna parameters has also been studied in the proposed work. The fabricated prototype antenna provides good impedance matching and circular polarization over the entire frequency range and is compact in size with a height of 0.078 wavelengths (λ_m) at the lowest frequency. The antenna exhibits a rotating radiation pattern with frequency in the azimuth direction, providing an almost constant beamwidth of 117°, with variation in gain limited to only 0.75 dBic above 8 GHz, yielding a flat gain response at higher frequencies. The compact size and improved parameters of the designed wideband antenna with a stepped reflector make it a suitable candidate for electronic warfare applications.

1. INTRODUCTION

A frequency-independent antenna is recognized for its wideband impedance matching, gain, and uniform radiation pattern over a wide range of frequencies. In the 1950s, the first spiral antenna was introduced based on the concept of a frequency-independent antenna [1]. Wide bandwidth, consistent input impedance, constant beamwidth, and circular polarization make the spiral antenna ideal for most wideband applications. Performance enhancement of antennas has been a demanding area of research for antenna designers for decades. Significant work has been carried out for the performance improvement of different frequency-independent antennas, but spiral antennas have received comparatively less attention.

A unidirectional beam is often desirable as it reduces interference from placement structures and improves antenna performance. Various techniques for improving the radiation properties over a wide band of frequencies have been explored in literature, like modifying the ground plane geometry, reactive loading, artificial materials [2, 3], magnetic materials [4, 5], lumped components [6], parasitic layers [7], etc. Absorbers are often placed under the antenna to improve the low-frequency response [8]. Novel methods have been used to design a compact spiral antenna over the 2–18 GHz frequency band. The maximum achievable bandwidth of a conductor-backed spiral antenna was calculated analytically as in [6]. Chip resistors have sometimes been integrated into the substrate to achieve a good axial ratio (AR) and high gain [9]. A polygonal spiral antenna has been placed inside a low-profile reflector to achieve a maximum gain of 6 dB [10]. Stepped reflector designs have been reported in [11, 12] to improve gain, and stepped absorbers have been used in [13] to improve AR at lower frequencies. A stepped reflector has been used in [15], where a significantly low gain is reported at a lower frequency. A study of numerically optimized conical conductive backing design for 2–10 GHz has been discussed in [16]. Another way of modifying conical conductive backing is by adding a step to form a modified backing where an improvement in gain has been observed [18]. For the above-discussed reflectors, there is gain and AR variation throughout the frequency band. To improve these parameters, a novel multistep reflector backing is proposed in this paper. A progressive development of the design is demonstrated to arrive at the recommended antenna geometry of the proposed spiral antenna with a stepped reflector, which improves its performance, yielding high gain, flat frequency response particularly above 8 GHz, and optimized AR at low frequencies for 2–18 GHz applications. A key focus of this work is achieving a flat gain response above 8 GHz, which is particularly important for wideband communication and sensing systems operating across the 8–18 GHz range. In such systems, consistent gain across frequency ensures uniform signal strength, minimizes spectral distortion, and contributes to reliable overall system performance. A flat gain profile also reduces frequency-dependent variation in the link budget, mitigates the effects of frequency-selective fading, and simplifies system calibration and post-processing. These benefits are especially relevant in applications such as radar, electronic warfare (EW), and high-data-rate communication, where wide instantaneous bandwidth and spectral efficiency are critical.

2. CONFIGURATION AND STUDY WITH DIFFERENT REFLECTORS BACKING DESIGN

The geometry of a spiral radiator and the reflector backing is shown in Fig. 1. The centerline of the spiral antenna is governed

* Corresponding author: Abhay M. Morey (mabhay22phd@student.mes.ac.in).

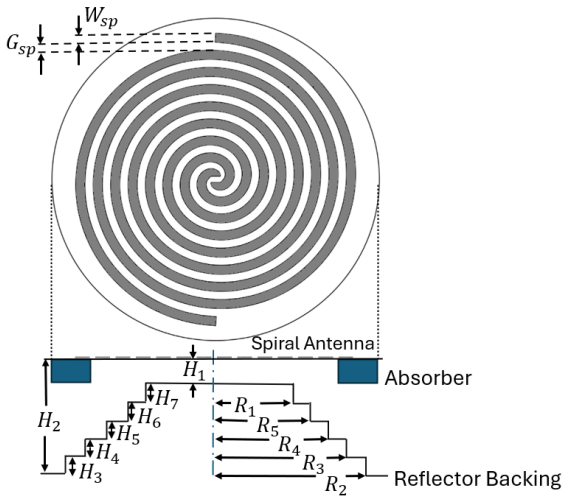

FIGURE 1. Schematic of the spiral antenna with stepped reflector.

by the Archimedean function as in Eq. (1) [18]

$$r_{sp} = a_{sp} \cdot \varphi_w \tag{1}$$

where r_{sp} = radius of spiral from the origin to center line of the arm, a_{sp} = 1.273 mm/rad the spiral constant, and φ_w = winding angle.

The reference antenna in Fig. 1 has eight turns, arm width $W_{sp} = 2.0$ mm, the separation between turns $G_{sp} = 2.0$ mm, and the substrate selected for simulation is Rogers RT/Duroid 5880 with epsilon $(\varepsilon_r) = 2.2$ and loss tangent $(\tan\delta) = 0.0009$ [13]. A commercially available flat absorber JV Micronics-JVMBF226 [14], with a height of 5 mm, a width of 10 mm, and an outer diameter of 78 mm, was placed under the antenna [15]. The antenna was excited with a discrete port impedance of 120 Ω [20]. The designed structure has been simulated using Dassault's CST Microwave Studio Suite 2021 software [21].

A balun is required to connect spiral antennas to a coaxial cable. When being operated in balanced mode, these antennas exhibit circular polarization. The arms of the spiral get equal amplitudes and opposite phases from balanced structures, which are symmetrical around the feeding point. The imbalanced output of the coaxial line can result in a skewed beam due to an imbalance in the current magnitude of the spiral arms. A balun generates a balanced differential output to help impedance matching between the spiral and coaxial lines.

The structure of the tapered feed balun top and bottom sides is shown in Fig. 2. The balun is printed on a Rogers RT Duroid 5880 substrate, which has a thickness of 1.57 mm, a ϵ_r value of 2.2, and a loss tangent $\tan\delta$ of 0.0009. The width of the top plane ($W_{tu} = 4.5$ mm) and bottom plane ($W_{bu} = 30$ mm) tapers gradually to the end ($W_{tb} = W_{bb} = 2.1$ mm) to form a balanced transmission line. These parallel trace lines are kept at a length of $L_b = 60$ mm.

2.1. Spiral Antenna over Flat Reflector

The spiral antenna has been simulated over a flat reflector at different heights, H, to study the active region of the spiral. The antenna starts to radiate as the circumference C of the spiral equals one wavelength $(C = \lambda)$, with each frequency being radiated near a radius $r = \frac{\lambda}{2\pi}$. This region is known as the active region [5]. A parameter Δg has been considered to understand the gain variation, where Δg = the difference between the maximum and minimum gains over the 8–18 GHz band [17]. Minimizing gain variation ensures a flatter gain response, allowing the antenna to maintain consistent performance across the entire operating band. This attribute is particularly critical in wideband applications, where signal integrity and uniformity over frequency directly impact system reliability and efficiency. Significant fluctuations in gain can result in uneven transmission or reception quality, potentially degrading overall system performance.

The simulated results are plotted in Fig. 3. It is seen from Fig. 3(a) that the gain of the reference antenna varies between 3.0 and 5.6 dBic over 2–18 GHz. The gain at lower frequencies improves when the flat conductor is placed at 12 mm, but gradually degrades as the height is reduced to 5 mm. At higher frequencies, a significant variation in gain is observed at 12 mm, but as the conductor is moved to 5 mm, the variation decreases, leading to improved gain stability. Low gain is observed at frequencies where the height $H = \frac{\lambda}{2}$. This phenomenon mainly occurs due to the reflected waves from the reflector causing destructive interference, leading to gain degradation [18]. As the wave travels towards the outer turn of the spiral, it scatters and reflects towards the feed, increasing the cross-polarization level and degrading the low-frequency AR [19] as shown in Fig. 3(b), where AR $>$ 3 dB below 2.75 GHz for the reference antenna and AR $<$ 3 dB is observed for all the different heights of the flat conductor. From this study, we have fixed the heights of $H_1 = 5$ mm and $H_2 = 12$ mm.

2.2. Spiral Antenna by Adding Steps to the Reflector

Combining the benefits of flat reflectors at various heights, a study has been performed by placing the antenna above a reflector with different numbers of steps. The number of steps was designed in such a way that their height and width were evenly distributed between the reflector's height H_1-H_2 and radius R_1-R_2, as shown in Fig. 1. The simulation results of the reflector with different step numbers are shown in Fig. 4. In the first case with one step reflector, it is observed that there is a gain improvement below 6 GHz, but after that, there is a significant drop in gain from 6–8 GHz. Thereafter, adding the second step, a gain improvement is seen at 6–8 GHz, but a drop is seen at higher frequencies. Adding the third and fourth steps, a stable gain has been achieved from 8–16 GHz, and a drop in gain above 16 GHz has been noticed. Adding the fifth step, a stable gain is achieved from the 8–18 GHz band, and at lower frequencies, the achieved gain shows a linearly increasing trend. After adding the sixth step, a drop in gain below 0 dBic at 2.5 GHz is observed, and a minimal drop in gain is seen from 14–18 GHz. However, the most uniform right hand circular polarization (RHCP) gain out of these, in the 8–18 GHz band, has been achieved by using a five-step reflector as shown in Fig. 1, with a $\Delta g = 0.75$ dBic and the gain varying between 8.0 and 8.75 dBic.

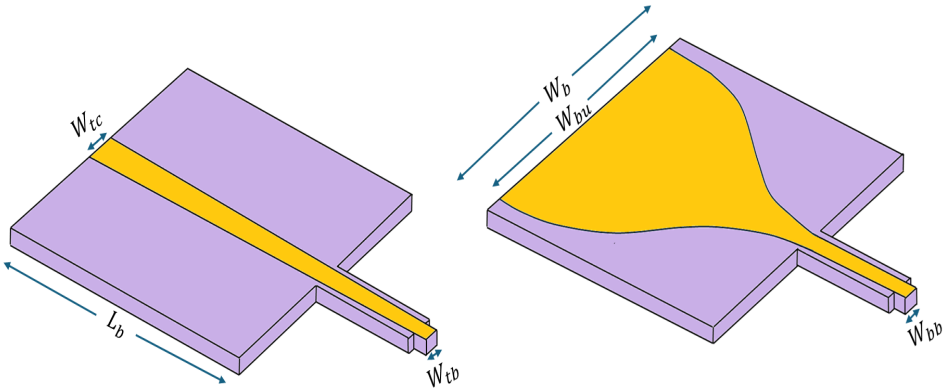

FIGURE 2. Geometry of tapered microstrip balun.

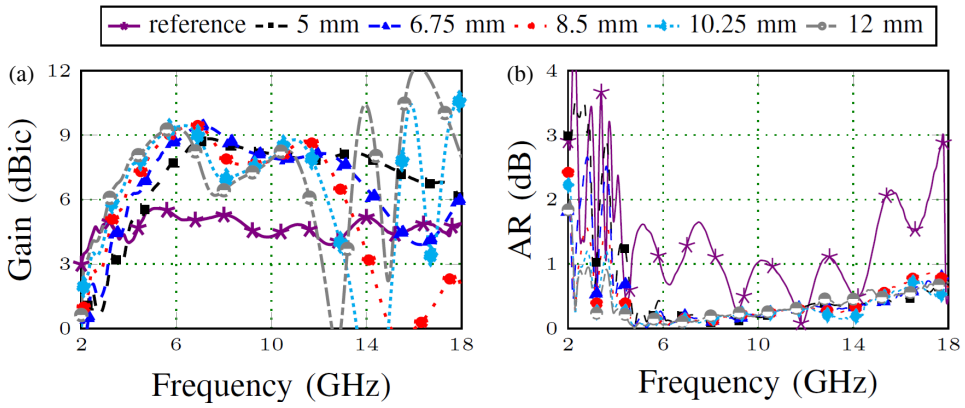

FIGURE 3. Parametric study by varying the height of the ground reflector: (a) Gain, (b) AR.

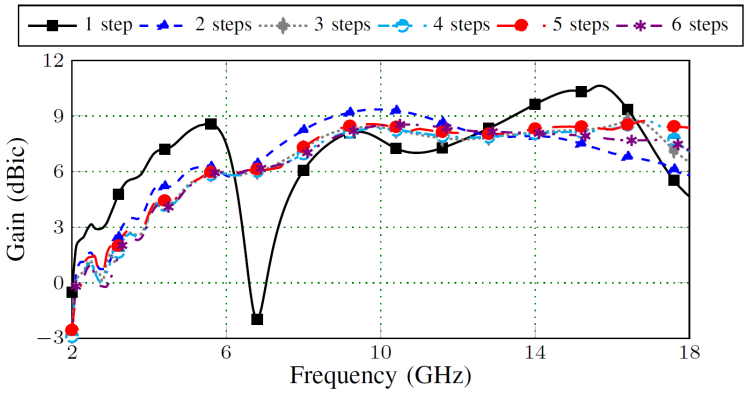

FIGURE 4. Simulated results for RHCP gain with different numbers of steps for the reflector.

2.3. Spiral Antenna over Multistep Reflector

For further improvement in Δg, the proposed multi-step reflector was modified by varying the step height and width to get the best suitable flat gain. Every time just one parameter out of these was varied, keeping all the other lengths equal, i.e., height 1.6 mm and length 4.8 mm. The width R_1 was varied from 6 mm to 9 mm as shown in Fig. 5(a), and height H_3 was varied from 1 mm to 2 mm as shown in Fig. 5(b). The results have been reproduced for widths of 6 mm, 7.75 mm, and 9 mm, and heights of 1 mm, 1.5 mm, and 2 mm. An improved Δg at $R_1 = 7.75$ mm and $H_3 = 1.5$ mm is observed from Fig. 5. Similarly, by varying the width and height of other steps over the respective ranges, an optimal Δg was achieved for each step as shown in Table 1.

2.4. Performance Improvement Compared to Other Reflectors

The performance of the spiral antenna with optimized dimensions of the reflector, as shown in Table 1, has been compared with the performance of spiral antennas over reflectors as found

TABLE 1. Optimized heights and widths of steps for the stepped ground reflector.

Step	Optimized width	Δg (dB)
R_1	7.75 mm	0.4
R_2	16.75 mm	0.3
R_3	14.75 mm	0.6
R_4	12.75 mm	0.6
R_5	10.75 mm	0.5

Step	Optimized height	Δg (dB)
H_3	1.5 mm	0.6
H_4	1.5 mm	0.6
H_5	1.3 mm	0.5
H_6	1.7 mm	0.4
H_7	1.5 mm	0.7

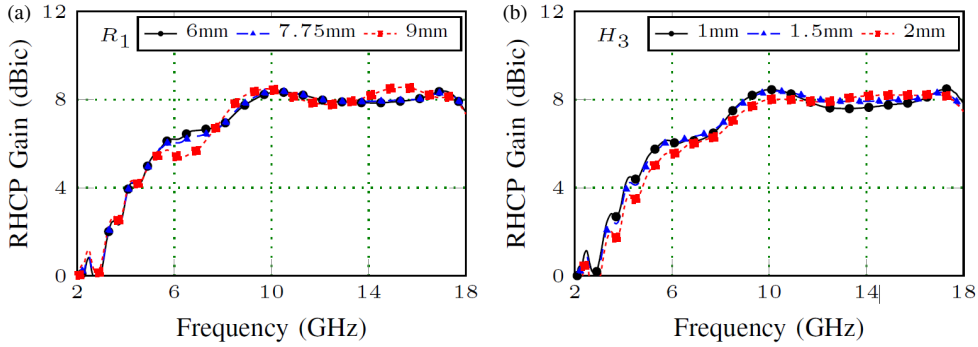

FIGURE 5. Parametric study by varying the step height and width of the stepped ground reflector.

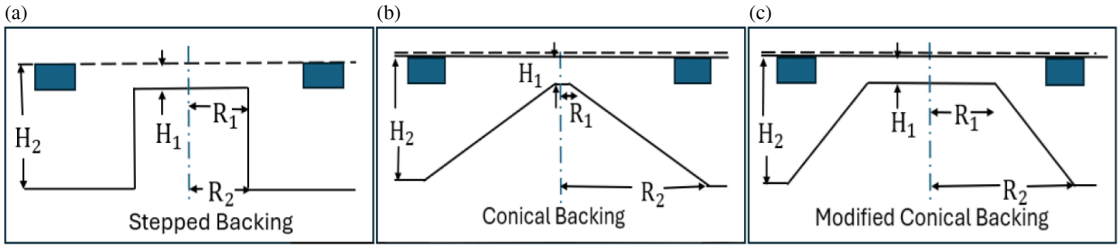

FIGURE 6. Schematic of the spiral antenna with (a) Stepped reflector [11]. (b) Conical reflector [15]. (c) Modified conical reflector [16].

in the literature. A spiral antenna placed over a step reflector structure as shown in Fig. 6(a) has been studied in [11], where the height $H_1 = 5$ mm and $H_2 = 12$ mm and $R_1 = 2.5$ mm. The simulated RHCP gain is shown in Fig. 7, where there is a drop in gain at 7 GHz. In [15], a conical backing was placed below the spiral antenna, as shown in Fig. 6(b), where H_1 and H_2 are the same as those of the stepped reflector in [11]. A conical shape has been formed between the two surfaces with radius $R_1 = 2.5$ mm, which allows sufficient space for the balun feed and with a radius $R_2 = 36$ mm, which is the outer dimension of the spiral antenna. The simulated RHCP gain is shown in Fig. 7.

There is a drop in gain at 7 GHz and 14 GHz. The spiral antenna has been placed over a modified conical reflector structure [17] as shown in Fig. 6(c), where the radius R_1 has been increased to 12 mm, and a hole of 2.5 mm is made over this surface to pass the balun feed, keeping other dimensions same. The simulated RHCP gain is shown in Fig. 7, where there is an improvement in gain as compared to the conical reflector at 14 GHz, and the gain that was degraded to 2 dBic is now improved to 6.4 dBic. Finally, the spiral antenna has been placed over the multistep reflector proposed in this work as shown in Fig. 1. The simulated result shows that there is an improvement in gain compared to the modified conical reflector, and a flat gain response is observed from 8–18 GHz as shown in Fig. 7. The comparison of the proposed work with similar work in the existing literature as described above is reported in Table 2. Compared to the published research, the proposed optimized antenna performs better than the existing techniques, demonstrating its effectiveness in the design of compact and wideband spiral antennas. The proposed antenna configuration is seen to yield a better Δg over a much wider 8–18 GHz band, with a better gain over the same band than other antennas operating over the 2–18 GHz band.

3. EXPERIMENTAL VALIDATION

From the above investigation, it is observed that reflector steps close to the feed have more effect on higher frequencies than those near the edges. Therefore, it should be possible to achieve

TABLE 2. Comparison with reported works.

Ref.	Frequency range (GHz)	Maximum gain	Minimum gain	Δg (dB)	Antenna Height
[3]	3–10	9 dBi	2.7 dBi	-	$0.09\lambda_m$
[5]	3–10	9 dBi	5 dBi	-	$0.07\lambda_m$
[9]	2–18	5.5 dBic	−5 dBic	9	$0.02\lambda_m$
[10]	2–18	6 dB	−2 dB	-	$0.11\lambda_m$
[14]	2.5–17.5	8 dB	−10 dB	4.5	$0.013\lambda_m$
[16]	2–18	8.6 dBic	−1.1 dB	2.8	$0.08\lambda_m$
P.W.	**2–18**	**8.75 dBic**	**−1.0**	**0.75**	**$0.078\lambda_m$**

P.W. = Proposed Work

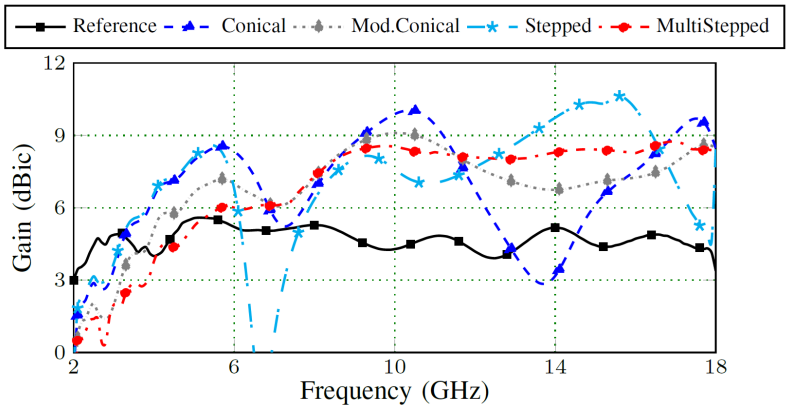

FIGURE 7. Comparison of a spiral antenna over various reflectors in literature to that over the developed multistep reflector.

a flat gain above 8 GHz by optimizing the radius of these steps, resulting in a multi-step reflector with improved gain and polarization performance. As per the above study H_1, H_2, H_3, H_4, H_5, H_6, H_7, R_1, R_2, R_3, R_4, and R_5, the dimensions given in Table 1 were found to be the optimum dimensions for prototyping the reflector of the spiral antenna.

A spiral antenna with uniform width, spacing of 2 mm, and diameter of 70 mm is fabricated using Rogers RT duroid 5880 ($\varepsilon_r = 2.2$, $\tan\delta = 0.0009$) with thickness 0.8 mm. Fig. 8(a)(i) shows the photograph of the fabricated spiral geometry, and Fig. 8(a)(ii) shows the absorber holding arrangement. The fabricated multistep reflector is shown in Fig. 8(a)(iii) where the top surface of the reflector is covered with the copper tape of a thickness of 0.08 mm to realize the perfect electric conductor (PEC) backing as in the simulation.

A tapered wideband planar balun is designed to match the spiral antenna impedance of 120 Ω to the standard input impedance of 50 Ω using the same substrate but with a thickness of 1.57 mm, and the height of the balun is 45 mm. The feed substrate width is reduced along the end to match the reflector hole of 2.5 mm and is fitted in the reflector. The balun is also covered with a 3D printed case with absorbing material, and the inner side is covered with copper tape and absorber as shown in Fig. 8(b)(i), to reduce the radiation from the feed. Fig. 8(b)(ii) shows the top view, while Fig. 8(b)(iii) illustrates the bottom view of the assembled spiral antenna.

Measurements were conducted on a Keysight FieldFox N9917A vector network analyzer (VNA). The measured and simulated results of the proposed antenna are shown in Fig. 9(a), where it is observed that $|S_{11}| < -10$ dB over the entire frequency range of 2–18 GHz. The radiation characteristics of the antenna were measured inside an anechoic chamber using the horn antenna as the reference. The RHCP (Right hand circularly polarized) and LHCP (Left hand circularly polarized) gains were calculated from the measured linear response of the horn antenna as shown in Figs. 9(b) and (c). The variation in RHCP gain is from −1.0 dBic to 8.75 dBic, and above 8 GHz, the gain response stays flat within 8–8.75 dBic with a Δg = 0.75 dB till 18 GHz. An excellent agreement is seen between the simulated and measured results.

The cross-polar LHCP gain is 15 dB below the RHCP gain over all the frequencies. The simulated and measured ARs are summarized in Fig. 9(d), where AR < 3 dB and circular polarization response are observed over a wide frequency band, and a good agreement is seen between the simulated and measured results. As shown in Fig. 10, the current distribution of the spiral antenna varies with frequency, highlighting the frequency-dependent behaviour of the structure. Specifically, by analysing the surface current distributions at repre-

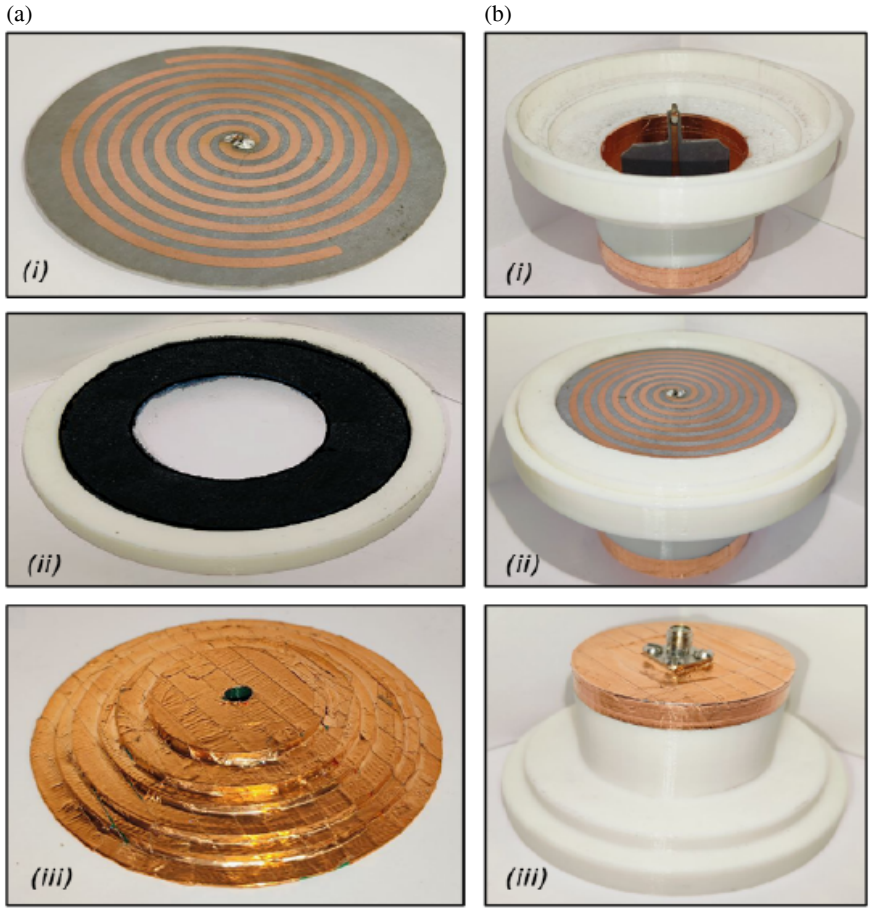

FIGURE 8. Fabricated prototype of (a) (i) spiral antenna, (ii) absorber on support, (iii) multistep Reflector backing, (b) (i) balun assembly, (ii) complete antenna assembly top, (iii) bottom antenna assembly.

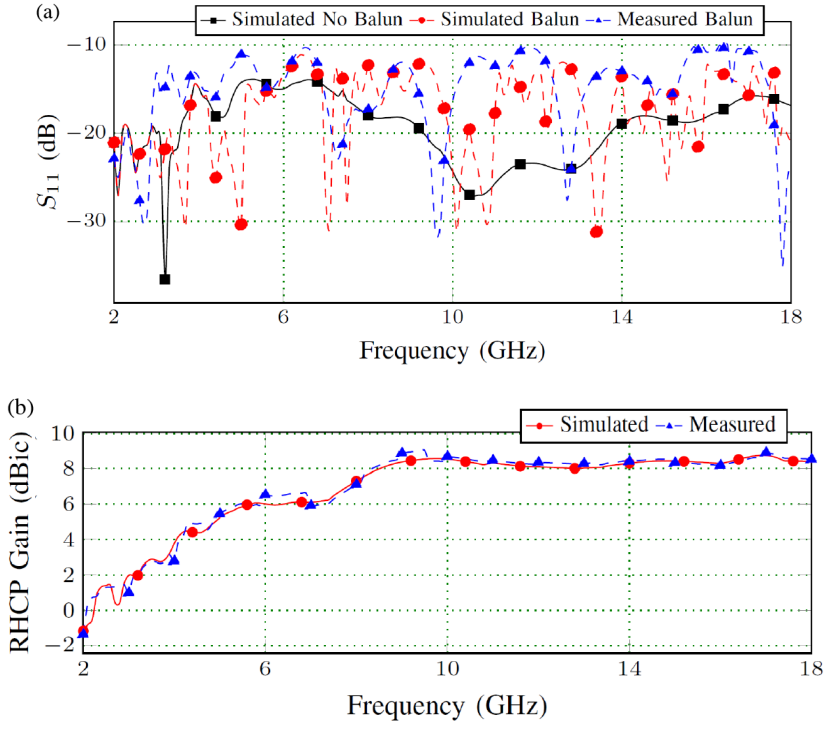

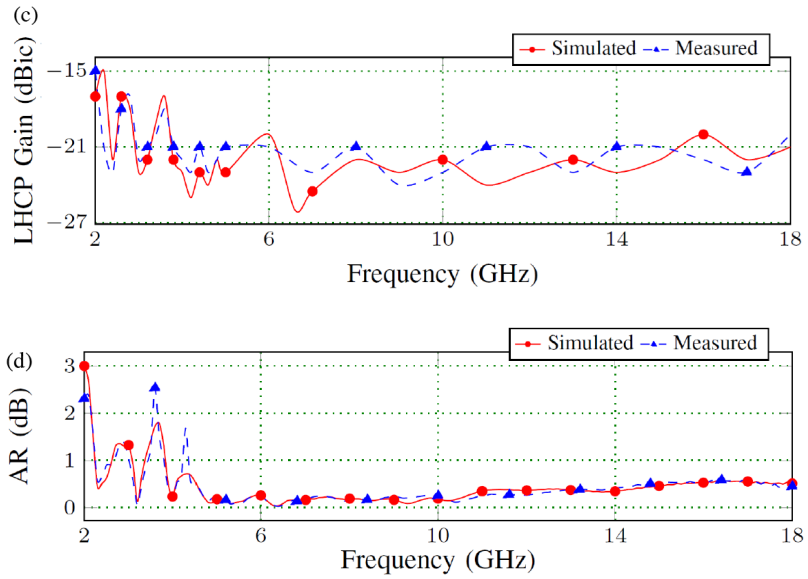

FIGURE 9. Simulated and measured (a) $|S_{11}|$, (b) boresight RHCP gain, (c) boresight LHCP gain, (d) boresight AR of the designed geometry.

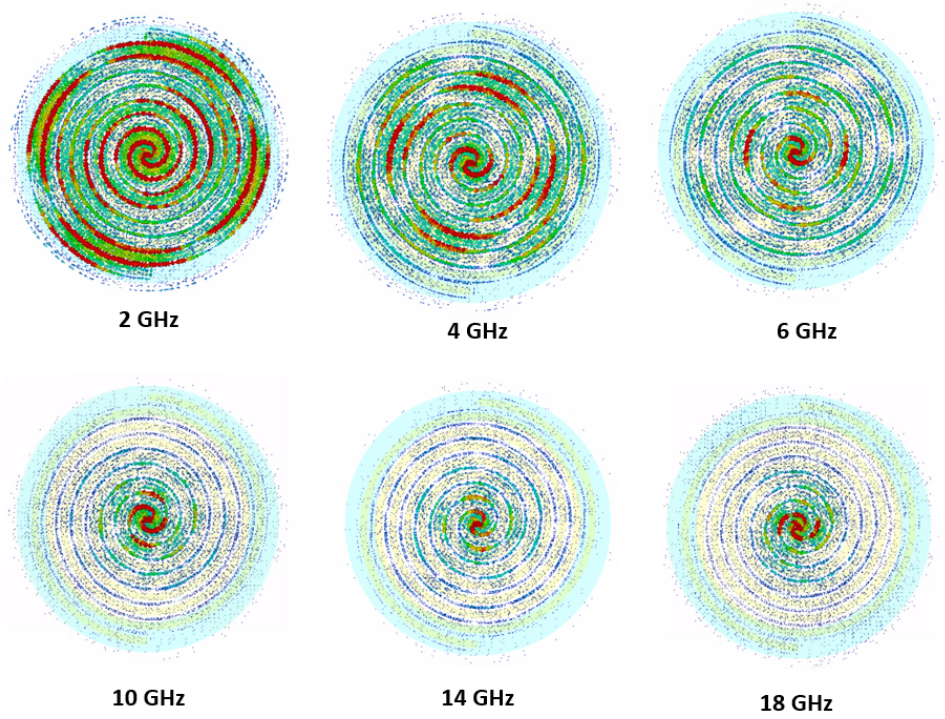

FIGURE 10. Current distribution of spiral antenna at various frequencies.

sentative frequencies across the 2–18 GHz band, we observe a clear frequency-dependent modal evolution. At lower frequencies (e.g., 2–4 GHz), the current is primarily concentrated near the outer turns of the spiral, indicating dominant mode-1 excitation. This results in a symmetric current pattern and a broad, stable radiation beam with good circular polarization. As frequency increases (e.g., 8–12 GHz), the active radiation region shifts inward, and the current becomes more concentrated and well centered, maintaining circular symmetry. At higher frequencies (e.g., 14–18 GHz), the current distribution becomes increasingly asymmetric, with evidence of counter-rotating currents and signatures of higher order mode excitation. Despite the emergence of higher-order modes, the axial ratio remains well controlled across the band, suggesting that the stepped cavity plays a critical role in managing these modal transitions.

The simulated and measured normalized radiation patterns in $\phi = 0°$ and $90°$ planes at different frequencies are plotted in Fig. 11. The radiation pattern of the antenna was measured using the setup illustrated in Fig. 12. The antenna under test was placed on a rotating platform within an anechoic chamber to minimize reflections and external interference. To

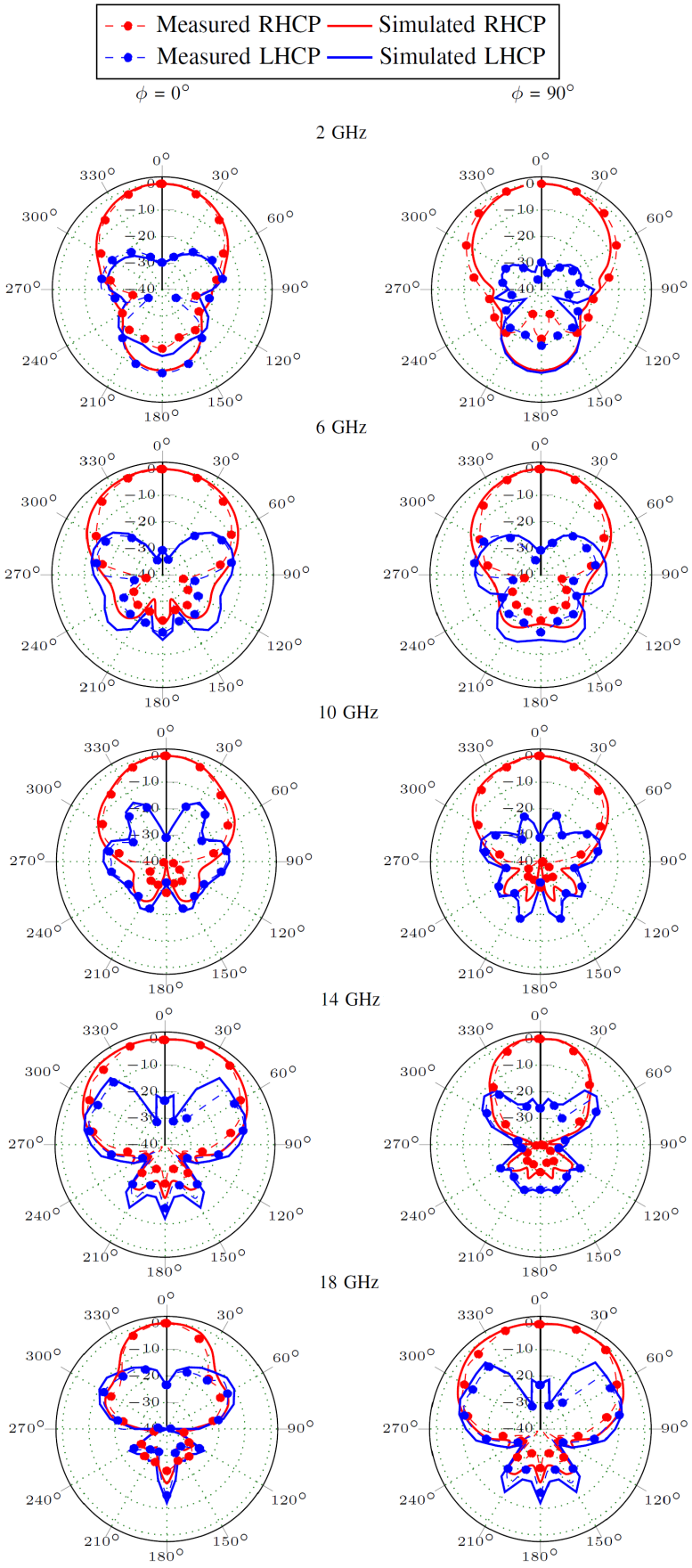

FIGURE 11. Measured and simulated normalized radiation patterns at different frequencies.

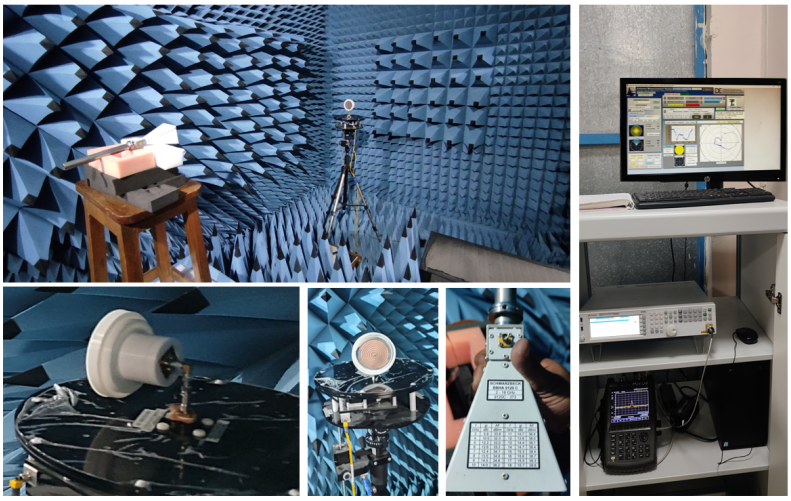

FIGURE 12. Radiation pattern measurement setup.

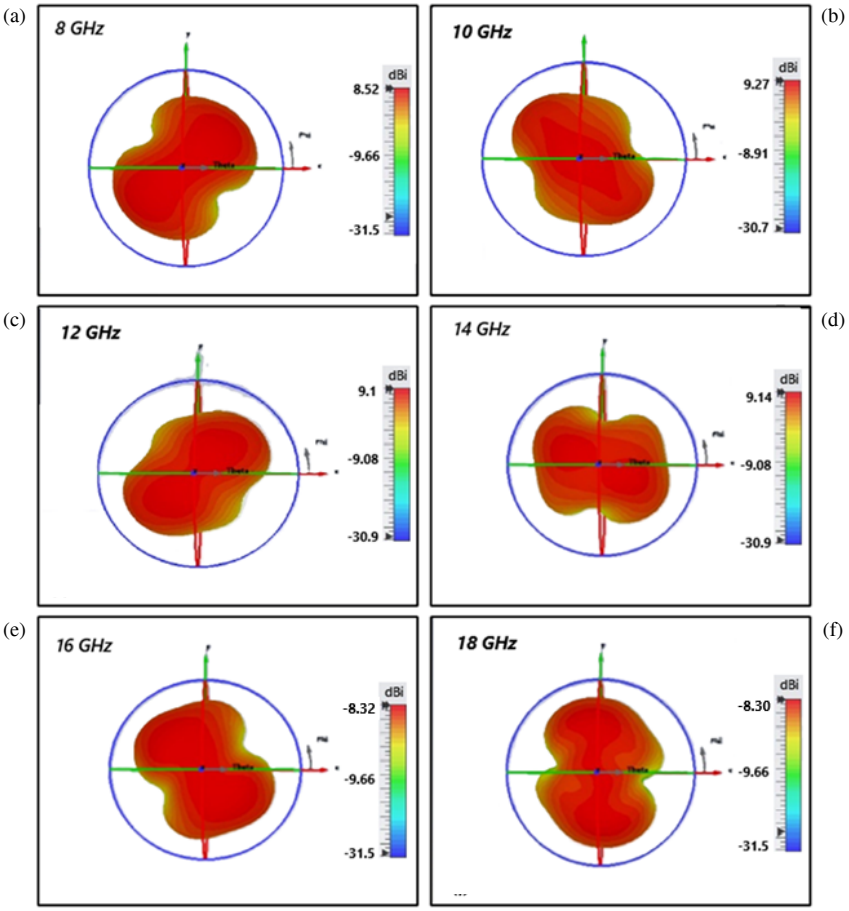

FIGURE 13. Rotating radiation pattern in azimuth for the proposed spiral antenna.

accurately characterize the antenna's performance across the 2–18 GHz band, a segmented measurement approach was employed using multiple standard gain horn antennas for 2–4 GHz, 4–8 GHz, and 8–18 GHz sub-bands. Each horn antenna had a low cross-polarization performance within its specific frequency range. This strategy effectively minimized the influence of polarization impurities from the transmitting antenna, ensuring the measured values closely reflect the intrinsic performance of the antenna under test. All measurements were carried out in a fully anechoic chamber, with precise mechanical alignment and polarization matching for each antenna used. This frequency-specific and carefully calibrated setup significantly improved the accuracy of the measurements, enabling the close agreement observed with simulations, performance

that would not have been possible using a single wideband transmitting antenna. The small difference observed may be due to the imperfection in the mounting of the antenna in the 3D-printed structure. The pattern is observed to rotate in the azimuth direction with frequency, because of which a constant beamwidth (and constant gain) is observed from 8–18 GHz, as shown in Fig. 13. The achieved cross-polarization level is between 15 and 26 dB. Due to this rotating radiation pattern, the beamwidth measured at fixed angles $\phi = 0°$ and $\phi = 90°$ varies from a minimum half-power beamwidth ($HPBW_{min}$) of 40° to a maximum ($HPBW_{max}$) of 117°, across the 2–18 GHz. The 3D radiation patterns reveal that the main beam exhibits a frequency-dependent rotation in the azimuth plane, while the beamwidth in both principal planes (rotating with frequency) remains nearly constant at approximately 117°, across the 8–18 GHz band, achieving a flat gain response above 8 GHz. Due to this phenomenon, this antenna can be used in either standalone or frequency-scanned array applications.

4. CONCLUSION

The gain variation of a frequency-independent wideband circularly polarized spiral antenna has been reduced by modifying a flat reflector structure to a multistepped one. A simulation study was performed over the multi-step conductive backing structure by varying the height and length of the steps, and the dimensions have been optimized to yield a low variation in gain over the 8–18 GHz band. A fabricated prototype was evaluated over 2–18 GHz, and a good agreement was observed between the measured and simulated results. Circular polarization and wideband matching were achieved throughout the band. The gain was observed to be positive above 2.3 GHz with a maximum value of 8.75 dBic at 17 GHz. The gain variation Δg was observed to be 0.75 dB over 8–18 GHz, providing a flat gain response. The radiation pattern was observed to rotate in the azimuth direction, making the beamwidth constant over the 8–18 GHz band, leading to a flat gain. A comparison with the published research demonstrates that the method proposed for optimized antenna performs better than the existing techniques used for designing compact and wideband spiral antennas. The spiral antenna proposed in this paper can be used in airborne, electronic warfare (EW) applications and for frequency-scanned array applications.

REFERENCES

[1] Turner, E. M., "Spiral slot antenna," *WADC, Aerial Reconnaissance Laboratory, Project*, Vol. 4341, 55–8, 1955.

[2] Amiri, M. A., C. A. Balanis, and C. R. Birtcher, "Gain and bandwidth enhancement of a spiral antenna using a circularly symmetric his," *IEEE Antennas and Wireless Propagation Letters*, Vol. 16, 1080–1083, 2017.

[3] Tanabe, M. and H. Nakano, "Low-profile wideband spiral antenna with a circular his reflector composed of homogenous fan-shaped patch elements," *IEEE Transactions on Antennas and Propagation*, Vol. 68, No. 10, 7219–7222, Oct. 2020.

[4] Tanabe, M., Y. Masuda, and H. Nakano, "Low-profile spiral antenna placed on an extremely thin magnetodielectric substrate," *IEEE Antennas and Wireless Propagation Letters*, Vol. 16, 2050–2053, 2017.

[5] Durbha, R. and M. N. Afsar, "Miniaturization techniques using magnetic materials for broadband antenna applications," *IEEE Transactions on Magnetics*, Vol. 55, No. 7, 1–7, Jul. 2019.

[6] Nakano, H., S. Sasaki, H. Oyanagi, and J. Yamauchi, "Cavity-backed Archimedean spiral antenna with strip absorber," *IET Microwaves, Antennas & Propagation*, Vol. 2, No. 7, 725–730, Oct. 2008.

[7] Liu, X., J.-P. Geng, X. Liang, R.-H. Jin, C. Zhang, and K. Wang, "An improvement to directional equiangular spiral antenna with wide CP band, high gain and low profile," *Progress In Electromagnetics Research C*, Vol. 48, 53–60, 2014.

[8] Djoma, C., M. Jousset, A. C. Lepage, S. Mallégol, C. Renard, and X. Begaud, "Maximal bandwidth of an Archimedean spiral antenna above a reflector," *IEEE Antennas and Wireless Propagation Letters*, Vol. 13, 333–336, 2014.

[9] Fu, W., E. R. Lopez, W. S. T. Rowe, and K. Ghorbani, "A planar dual-arm equiangular spiral antenna," *IEEE Transactions on Antennas and Propagation*, Vol. 58, No. 5, 1775–1779, May 2010.

[10] Rahman, N. and M. N. Afsar, "A novel modified archimedean polygonal spiral antenna," *IEEE Transactions on Antennas and Propagation*, Vol. 61, No. 1, 54–61, Jan. 2013.

[11] Rao, P. H., M. Sreenivasan, and L. Naragani, "Dual band planar spiral feed backed by a stepped ground plane cavity for satellite boresight reference antenna applications," *IEEE Transactions on Antennas and Propagation*, Vol. 57, No. 12, 3752–3756, Dec. 2009.

[12] Djoma, C., X. Begaud, A. C. Lepage, S. Mallégol, and M. Jousset, "Wideband stepped reflector for Archimedean spiral antenna," in *Proceedings of the 2012 IEEE International Symposium on Antennas and Propagation*, 1–2, Chicago, IL, USA, 2012.

[13] Chen, L.-L., L. Chang, Z.-Z. Chen, and Q.-N. Qiu, "Bandwidth-enhanced circularly polarized spiral antenna with compact size," *IEEE Access*, Vol. 8, 41 246–41 253, 2020.

[14] JV Micronics, "Flat multilayer broadband absorber," JVMBF226, www.jvmicronics.com.

[15] Afsar, M. N., Y. Wang, and D. Hanyi, "A new wideband cavity-backed spiral antenna," in *IEEE Antennas and Propagation Society International Symposium. 2001 Digest. Held in conjunction with: USNC/URSI National Radio Science Meeting (Cat. No.01CH37229)*, Vol. 4, 124–127, Boston, MA, USA, 2001.

[16] Acree, M. A. and A. Prata, "Archimedean spiral-mode microstrip antenna with improved axial ratio," in *IEEE Antennas and Propagation Society International Symposium. 1999 Digest. Held in conjunction with: USNC/URSI National Radio Science Meeting (Cat. No.99CH37010)*, Vol. 2, 1232–1235, Orlando, FL, USA, 1999.

[17] Roy, A., K. J. Vinoy, N. Martin, C. Quendo, and S. Mallégol, "Performance enhancement of a compact Archimedean spiral antenna for 2–18 GHz," in *2021 IEEE International Symposium on Antennas and Propagation and USNC-URSI Radio Science Meeting (APS/URSI)*, 289–290, Singapore, Dec. 2021.

[18] Buck, M. C. and D. S. Filipovic, "Spiral cavity backing effects on pattern symmetry and modal contamination," *IEEE Antennas and Wireless Propagation Letters*, Vol. 5, 243–246, 2006.

[19] Balanis, C. A., *Frequency Independent Antennas and Antenna Miniaturization*, 545–550, Wiley, 2009.

[20] Klopfenstein, R. W., "A transmission line taper of improved design," *Proceedings of the IRE*, Vol. 44, No. 1, 31–35, Jan. 1956.

[21] Dassault Systèmes, "CST microwave studio®," version 2021, Software.